Remnant PbI2, an unforeseen necessity in high-efficiency hybrid perovskite-based solar cells?a)

Duyen H. Cao, Constantinos C. Stoumpos, Christos D. Malliakas, Michael J. Katz, Omar K. Farha, Joseph T. Hupp, and Mercouri G. Kanatzidis

Citation: APL Materials **2**, 091101 (2014); doi: 10.1063/1.4895038
View online: http://dx.doi.org/10.1063/1.4895038
View Table of Contents: http://scitation.aip.org/content/aip/journal/aplmater/2/9?ver=pdfcov
Published by the AIP Publishing

APL MATERIALS **2**, 091101 (2014)

Remnant PbI_2, an unforeseen necessity in high-efficiency hybrid perovskite-based solar cells?[a]

Duyen H. Cao,[1] Constantinos C. Stoumpos,[1] Christos D. Malliakas,[1] Michael J. Katz,[1] Omar K. Farha,[1,2] Joseph T. Hupp,[1,b] and Mercouri G. Kanatzidis[1,b]

[1]*Department of Chemistry, and Argonne-Northwestern Solar Energy Research (ANSER) Center, Northwestern University, 2145 Sheridan Road, Evanston, Illinois 60208, USA*
[2]*Department of Chemistry, Faculty of Science, King Abdulaziz University, Jeddah, Saudi Arabia*

(Received 2 May 2014; accepted 26 August 2014; published online 18 September 2014)

Perovskite-containing solar cells were fabricated in a two-step procedure in which PbI_2 is deposited via spin-coating and subsequently converted to the $CH_3NH_3PbI_3$ perovskite by dipping in a solution of CH_3NH_3I. By varying the dipping time from 5 s to 2 h, we observe that the device performance shows an unexpectedly remarkable trend. At dipping times below 15 min the current density and voltage of the device are enhanced from 10.1 mA/cm^2 and 933 mV (5 s) to 15.1 mA/cm^2 and 1036 mV (15 min). However, upon further conversion, the current density decreases to 9.7 mA/cm^2 and 846 mV after 2 h. Based on X-ray diffraction data, we determined that remnant PbI_2 is always present in these devices. Work function and dark current measurements showed that the remnant PbI_2 has a beneficial effect and acts as a blocking layer between the TiO_2 semiconductor and the perovskite itself reducing the probability of back electron transfer (charge recombination). Furthermore, we find that increased dipping time leads to an increase in the size of perovskite crystals at the perovskite-hole-transporting material interface. Overall, approximately 15 min dipping time (∼2% unconverted PbI_2) is necessary for achieving optimal device efficiency. [http://dx.doi.org/10.1063/1.4895038]

With the global growth in energy demand and with compelling climate-related environmental concerns, alternatives to the use of non-renewable and noxious fossil fuels are needed.[1] One such alternative energy resource, and arguably the only legitimate long-term solution, is solar energy. Photovoltaic devices which are capable of converting the photon flux to electricity are one such device.[2] Over the last 2 years, halide hybrid perovskite-based solar cells with high efficiency have engendered enormous interest in the photovoltaic community.[3,4] Among the perovskite choices, methylammonium lead iodide ($MAPbI_3$) has become the archetypal light absorber. Recently, however, Sn-based perovskites have been successfully implemented in functional solar cells.[5,6] $MAPbI_3$ is an attractive light absorber due to its extraordinary absorption coefficient of 1.5×10^4 cm^{-1} at 550 nm;[7] it would take roughly 1 μm of material to absorb 99% of the flux at 550 nm. Furthermore, with a band gap of 1.55 eV (800 nm), assuming an external quantum efficiency of 90%, a maximum current density of ca. 23 mA/cm^2 is attainable with $MAPbI_3$.

Recent reports have commented on the variability in device performance as a function of perovskite layer fabrication.[8] In our laboratory, we too have observed that seemingly identical films

[a]Invited for the Perovskite Solar Cells special topic.
[b]Authors to whom correspondence should be addressed. Electronic addresses: j-hupp@northwestern.edu and m-kanatzidis@northwestern.edu

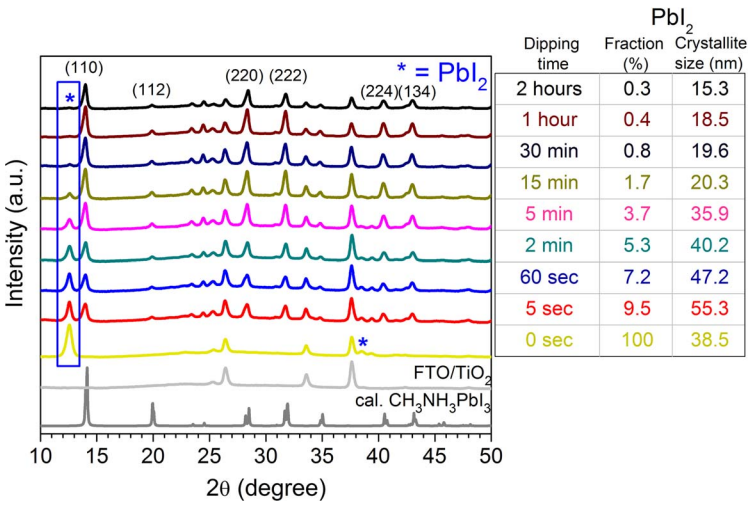

Dipping time	PbI_2 Fraction (%)	PbI_2 Crystallite size (nm)
2 hours	0.3	15.3
1 hour	0.4	18.5
30 min	0.8	19.6
15 min	1.7	20.3
5 min	3.7	35.9
2 min	5.3	40.2
60 sec	7.2	47.2
5 sec	9.5	55.3
0 sec	100	38.5

FIG. 1. X-ray diffraction patterns of $CH_3NH_3PbI_3$ films with increasing dipping time (% composition of PbI_2 was determined by Rietveld analysis (see Sec. S3 of the supplementary material for the Rietveld analysis details).

have markedly different device performance. For example, when our films of PbI_2 are exposed to MAI for several seconds (ca. 60 s), then a light brown colored film is obtained rather than the black color commonly observed for bulk $MAPbI_3$ (see Sec. S2 of the supplementary material for the optical band gap of bulk $MAPbI_3$).[23] This brown color suggests only partial conversion to $MAPbI_3$ and yields solar cells exhibiting a J_{sc} of 13.4 mA/cm^2 and a V_{oc} of 960 mV; these values are significantly below the 21.3 mA/cm^2 and 1000 mV obtained by others.[4] Under the hypothesis that fully converted films will achieve optimal light harvesting efficiency, we increased the conversion time from seconds to 2 h. Unexpectedly, the 2-h dipping device did not show an improved photovoltaic response (J_{sc} = 9.7 mA/cm^2, V_{oc} = 846 mV) even though conversion to $MAPbI_3$ appeared to be complete. With the only obvious difference between these two devices being the dipping time, we hypothesized that the degree of conversion of PbI_2 to the $MAPbI_3$ perovskite is an important parameter in obtaining optimal device performance. We thus set out to understand the correlation between the method of fabrication of the $MAPbI_3$ layer, the precise chemical compositions, and both the physical and photo-physical properties of the film. We report here that remnant PbI_2 is crucial in forming a barrier layer to electron interception/recombination leading to optimized J_{sc} and V_{oc} in these hybrid perovskite-based solar cells.

We constructed perovskite-containing devices using a two-step deposition method according to a reported procedure with some modifications.[4] (see Sec. S1 of the supplementary material for the experimental details).[23] $MAPbI_3$-containing photo-anodes were made by varying the dipping time of the PbI_2-coated photo-anode in MAI solution. In order to minimize the effects from unforeseen variables, care was taken to ensure that all films were prepared in an identical manner. The compositions of final $MAPbI_3$-containing films were monitored by X-ray diffraction (XRD). Independently of the dipping times, only the β-phase of the $MAPbI_3$ is formed (Figure 1).[9] However, in addition to the β-phase, all films also showed the presence of unconverted PbI_2 (Figure 1, marked with *) which can be most easily observed via the (*001*) and (*003*) reflections at $2\theta = 12.56^\circ$ and 38.54° respectively. As the dipping time is increased, the intensities of PbI_2 reflections decrease with a concomitant increase in the $MAPbI_3$ intensities. In addition to the decrease in peak intensities of PbI_2, the peak width increases as the dipping time increases indicating that the size of the PbI_2 crystallites is decreasing, as expected, and the converse is observed for the $MAPbI_3$ reflections. This observation suggests that the conversion process begins from the surface of the PbI_2 crystallites and proceeds toward the center where the crystallite domain size of the $MAPbI_3$ phase increases and that of PbI_2 diminishes. Interestingly, the remnant PbI_2 phase can be seen in the data of other reports, but has not been identified as a primary source of variability in cell performance.[8,10]

Considering that the perovskite is the primary light absorber within the device, we wanted to further investigate how the optical absorption of the film changes with increasing dipping time

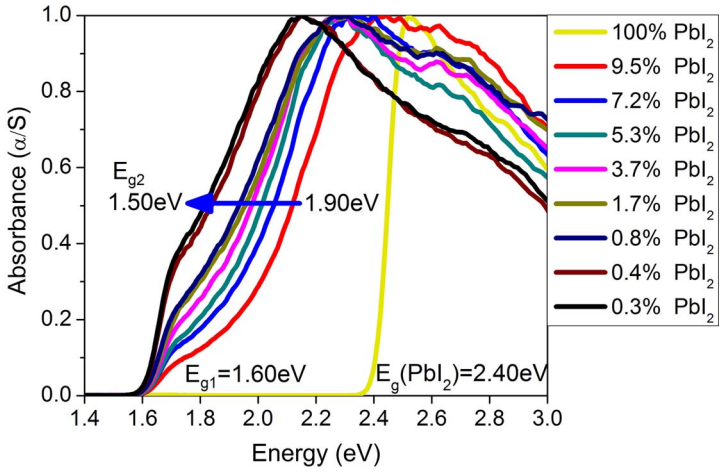

FIG. 2. Absorption spectra of $CH_3NH_3PbI_3$ films as a function of unconverted PbI_2 phase fraction.

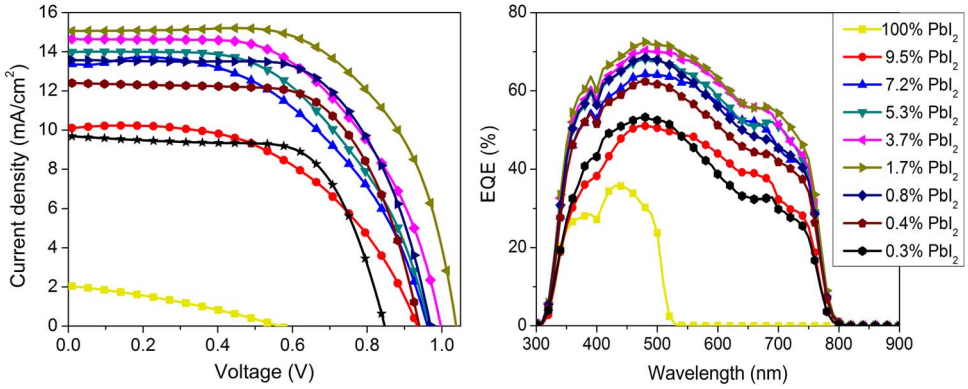

FIG. 3. (a) J-V curves and (b) EQE of $CH_3NH_3PbI_3$-based devices as a function of unconverted PbI_2 phase fraction.

(Figure 2).[11,12] The pure PbI_2 film shows a band gap of 2.40 eV, consistent with the yellow color of PbI_2. As the PbI_2 film is gradually converted to the perovskite, the band gap is progressively shifted toward 1.60 eV. The deviation of $MAPbI_3$'s band gap (1.60 eV) from that of the bulk $MAPbI_3$ material (1.55 eV) could be explained by quantum confinement effects related with the sizes of TiO_2 and $MAPbI_3$ crystallites and their interfacial interaction.[13,14] Interestingly, we also noticed the presence of a second absorption in the light absorber layer, in which the gap gradually red shifts from 1.90 eV to 1.50 eV as the PbI_2 concentration is decreased from 9.5% to 0.3% (Figure 2—blue arrow).

Having established the chemical compositions and optical properties of the light absorber films, we proceeded to examine the photo-physical responses of the corresponding functional devices in order to determine how the remnant PbI_2 affects device performance. The pure PbI_2 based device remarkably achieved a 0.4% efficiency with a J_{sc} of 2.1 mA/cm^2 and a V_{oc} of 564 mV (Figure 3(a)). Upon progressive conversion of the PbI_2 layer to $MAPbI_3$, we observe two different regions (Figure 4, Table I). In the first region, the expected behavior is observed; as more PbI_2 is converted to $MAPbI_3$, the trend is toward higher photovoltaic efficiency, due both to J_{sc} and V_{oc}, until 1.7% PbI_2 is reached. The increase in J_{sc} is attributable, at least in part, to increasing absorption of light by the perovskite. We speculate that progressive elimination of PbI_2, present as a layer between TiO_2 and the perovskite, also leads to higher net yields for electron injection into TiO_2 and therefore, higher J values. For a sufficiently thick PbI_2 spacer layer, electron injection would occur in stepwise fashion, i.e., perovskite $\rightarrow PbI_2 \rightarrow TiO_2$. Finally, the photovoltage increase is attributable to

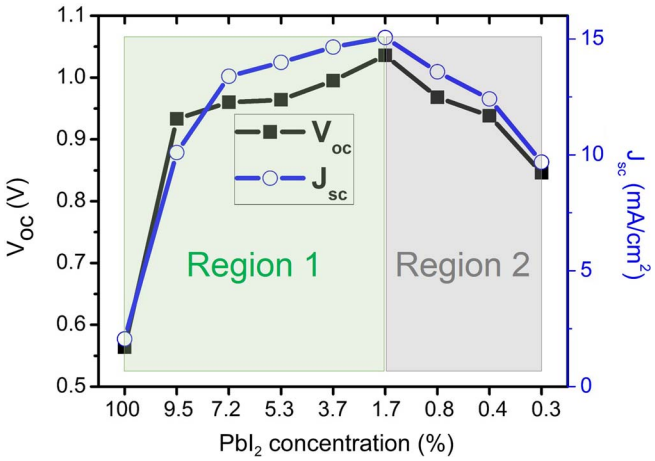

FIG. 4. Summary of J-V data vs. PbI_2 concentration of $CH_3NH_3PbI_3$-based devices (Region 1: 0 to 15 min dipping time, Region 2: 15 min to 2 h dipping time).

TABLE I. Photovoltaic performance of $CH_3NH_3PbI_3$-based devices as a function of unconverted PbI_2 fraction.

Dipping time	PbI_2 concentration[a]	J_{sc} (mA/cm^2)	V_{oc} (V)	Fill factor (%)	Efficiency (%)
0 s	100%	2.1	0.564	32	0.4
5 s	9.5%	10.1	0.933	52	4.9
60 s	7.2%	13.4	0.960	52	6.7
2 min	5.3%	14.0	0.964	55	7.4
5 min	3.7%	14.7	0.995	57	8.3
15 min	1.7%	15.1	1.036	62	9.7
30 min	0.8%	13.6	0.968	64	8.5
1 h	0.4%	12.4	0.938	65	7.6
2 h	0.3%	9.7	0.846	68	5.5

[a]Determined from the Rietveld analysis of X-ray diffraction data.

the positive shift in TiO_2's quasi-Fermi level as the population of photo-injected electrons is higher with increased concentration of $MAPbI_3$.

The second region yields a notably different trend; surprisingly, below a concentration of 2% PbI_2, J_{sc}, V_{oc}, and ultimately η decrease. Considering that the light-harvesting efficiency would increase when the remaining 2% PbI_2 is converted to $MAPbI_3$ (albeit to only a small degree), then the remnant PbI_2 must have some other role. We posit that remnant PbI_2 serves to inhibit detrimental electron-transfer processes (Figure 5). Two such processes are back electron transfer from TiO_2 to holes in the valence band of the perovskite (charge-recombination) or to the holes in the HOMO of the HTM (charge-interception). This retardation of electron interception/recombination observation is reminiscent of the behavior of atomic layer deposited Al_2O_3/ZrO_2 layers that have been employed in dye-sensitized solar cells.[15–18]

It is conceivable that the conversion of PbI_2 to $MAPbI_3$ occurs from the solution interface toward the TiO_2/PbI_2 interface and thus would leave sandwiched between TiO_2 and $MAPbI_3$ a blocking layer of PbI_2 that inhibits charge-interception/recombination. For this hypothesis to be correct, it is crucial that the conduction-band-edge energy (E_{cb}) of the PbI_2 be higher than the E_{cb} of the TiO_2.[19–21] The work function of PbI_2 was measured by ultraviolet photoelectron spectroscopy (UPS) and was observed to be at 6.35 eV vs. vacuum level, which is 0.9 eV lower than the valence-band-edge energy (E_{vb}) of $MAPbI_3$ (see Sec. S7 of the supplementary material[23] for the work function of PbI_2); the E_{cb} (4.05 eV) was calculated by subtracting the work function from the band gap (2.30 eV).

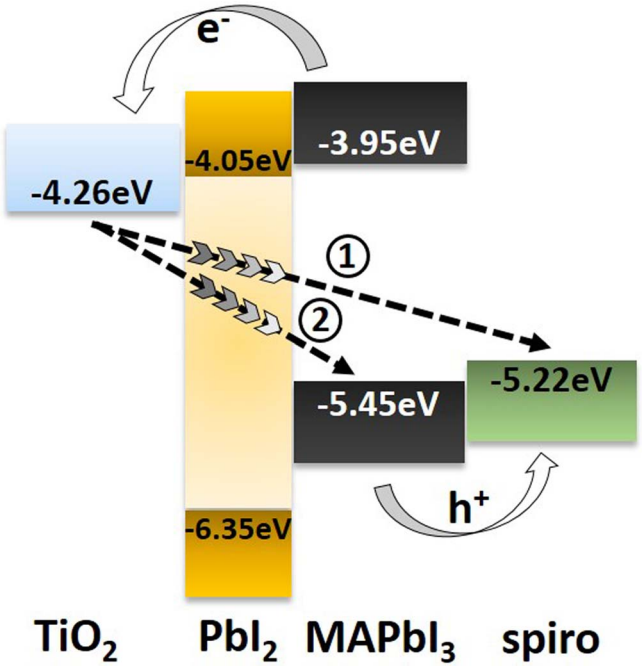

FIG. 5. Model of charge-interception/recombination retardation by the unconverted PbI_2 layer in $CH_3NH_3PbI_3$-based solar cell.

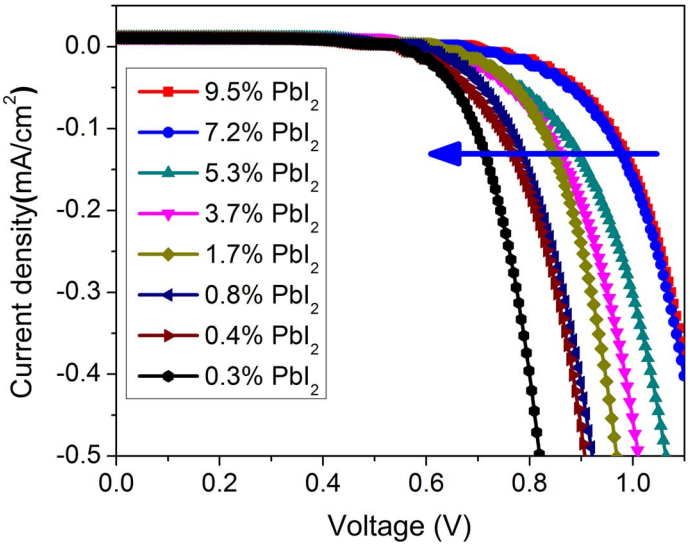

FIG. 6. Dark current of $CH_3NH_3PbI_3$-based devices as a function of unconverted PbI_2 phase fraction.

The E_{cb} of PbI_2 is 0.26 eV higher than the E_{cb} of TiO_2 and thus PbI_2 satisfies the conditions of a charge-recombination/interception barrier layer.

In order to probe the hypothesis that PbI_2 acts as a charge-interception barrier, dark current measurements, in which electrons flow from TiO_2 to the HOMO of the HTM, were made. Consistent with our hypothesis, Figure 6 illustrates that the onset of the dark current occurs at lower potentials as the PbI_2 concentration decreases. In the absence of other effects, the increasing dark current with increasing fraction of perovskite (and decreasing fraction of PbI_2) should result in progressively lower open-circuit photovoltages. Instead, the photocurrent density and the open-circuit photovoltage both increase, at least until to PbI_2 fraction reaches 1.7%. As discussed above, thinning of a PbI_2-based

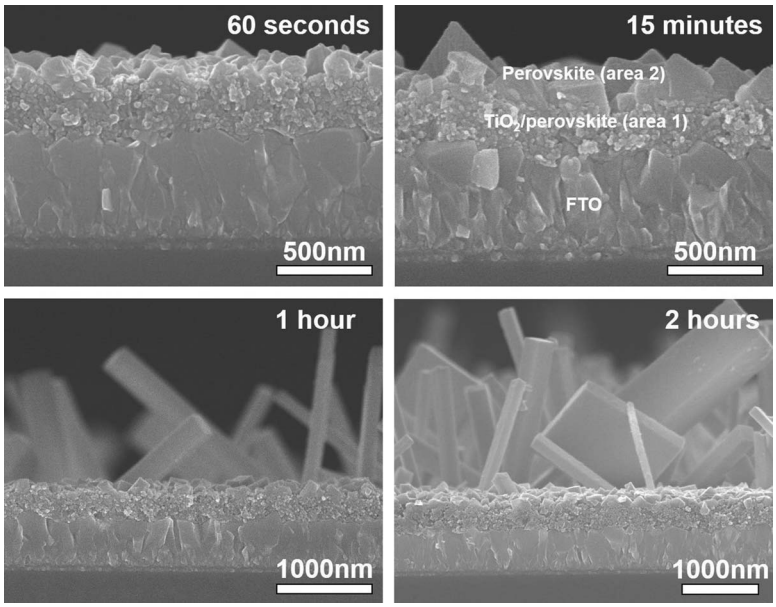

FIG. 7. Cross-sectional SEM images of $CH_3NH_3PbI_3$ film with different dipping time.

sandwich layer should lead to higher net injection yields, but excessive thinning would diminish the effectiveness of PbI_2 as a barrier layer for back electron transfer reactions.

Given the surprising role of remnant PbI_2 in these devices, we further probed the two-step conversion process by using scanning-electron microscopy (SEM) (Figure 7). Two domains of lead-containing materials (PbI_2 and $MAPbI_3$) are present. The first domain is sited within the mesoporous TiO_2 network (area 1) while the second grows on top of the network (area 2). Area 2 initially contains 200 nm crystals. As the dipping time is increased, the crystals show marked changes in size and morphology. The formation of bigger perovskite crystals is likely the result of the thermodynamically driven Ostwald ripening process, i.e., smaller perovskite crystals dissolves and re-deposits onto larger perovskite crystals.[22] The rate of charge-interception, as measured via dark current, is proportional to the contact area between the perovskite and the HTM. Thus, the eventual formation of large, high-aspect-ratio crystals, as shown in Figure 7, may well lead to increases in contact area and thereby contributes to the dark-current in Figure 6. Regardless, we found that the formation of large perovskite crystals greatly decreased our success rate in constructing high-functioning, non-shorting solar cells.

In summary, residual PbI_2 appears to play an important role in boosting overall efficiencies for $CH_3NH_3PbI_3$-containing photovoltaics. PbI_2's role appears to be that of a TiO_2-supported blocking layer, thereby slowing rates of electron(TiO_2)/hole(perovskite) recombination, as well as decreasing rates of electron interception by the hole-transporting material. Optimal performance for energy conversion is observed when ca. 98% of the initially present PbI_2 has been converted to the perovskite. Conversion to this extent requires about 15 min. Pushing beyond 98% (and beyond 15 min of reaction time) diminishes cell performance and diminishes the success rate in constructing non-shorting cells. The latter problem is evidently a consequence of conversion of small and more-or-less uniformly packed perovskite crystallites to larger, poorly packed crystallites of varying shape and size. Finally, the essential, but previously unrecognized, role played by remnant PbI_2 provides an additional explanation for why cells prepared dissolving and then depositing pre-formed $CH_3NH_3PbI_3$ generally under-perform those prepared via the intermediacy of PbI_2.

We thank Prof. Tobin Marks for use of the solar simulator and EQE measurement system. Electron microscopy was done at the Electron Probe Instrumentation Center (EPIC) at Northwestern University. Ultraviolet Photoemission Spectroscopy was done at the Keck Interdisciplinary Surface Science facility (Keck-II) at Northwestern University. This research was supported as part of the

ANSER Center, an Energy Frontier Research Center funded by the U.S Department of Energy, Office of Science, Office of Basic Energy Sciences, under Award No. DE-SC0001059.

[1] R. Monastersky, Nature (London) **497**(7447), 13 (2013).
[2] H. J. Snaith, J. Phys. Chem. Lett. **4**(21), 3623 (2013).
[3] M. M. Lee, J. Teuscher, T. Miyasaka, T. N. Murakami, and H. J. Snaith, Science **338**(6107), 643 (2012).
[4] J. Burschka, N. Pellet, S. J. Moon, R. Humphry-Baker, P. Gao, M. K. Nazeeruddin, and M. Gratzel, Nature (London) **499**(7458), 316 (2013).
[5] F. Hao, C. C. Stoumpos, D. H. Cao, R. P. H. Chang, and M. G. Kanatzidis, Nat. Photonics **8**(6), 489 (2014); F. Hao, C. C. Stoumpos, R. P. H. Chang, and M. G. Kanatzidis, J. Am. Chem. Soc. **136**, 8094–8099 (2014).
[6] N. K. Noel, S. D. Stranks, A. Abate, C. Wehrenfennig, S. Guarnera, A. Haghighirad, A. Sadhanala, G. E. Eperon, M. B. Johnston, A. M. Petrozza, L. M. Herz, and H. J. Snaith, Energy Environ. Sci. **7**, 3061 (2014).
[7] H. S. Kim, C. R. Lee, J. H. Im, K. B. Lee, T. Moehl, A. Marchioro, S. J. Moon, R. Humphry-Baker, J. H. Yum, J. E. Moser, M. Gratzel, and N. G. Park, Sci. Rep. **2**, 591 (2012).
[8] D. Y. Liu and T. L. Kelly, Nat. Photonics **8**(2), 133 (2014).
[9] C. C. Stoumpos, C. D. Malliakas, and M. G. Kanatzidis, Inorg. Chem. **52**(15), 9019 (2013).
[10] J. H. Noh, S. H. Im, J. H. Heo, T. N. Mandal, and S. I. Seok, Nano Lett. **13**(4), 1764 (2013).
[11] Diffuse reflectance measurements of $MAPbI_3$ films were converted to absorption spectra using the Kubelka-Munk equation, $\alpha/S = (1\text{-}R)^2/2R$, where R is the percentage of reflected light, and α and S are the absorption and scattering coefficients, respectively. The band gap values are the energy value at the intersection point of the absorption spectrum's tangent line and the energy axis.
[12] L. F. Gate, Appl. Opt. **13**(2), 236 (1974).
[13] O. Voskoboynikov, C. P. Lee, and I. Tretyak, Phys. Rev. B **63**(16), 165306 (2001).
[14] X. X. Xue, W. Ji, Z. Mao, H. J. Mao, Y. Wang, X. Wang, W. D. Ruan, B. Zhao, and J. R. Lombardi, J. Phys. Chem. C **116**(15), 8792 (2012).
[15] E. Palomares, J. N. Clifford, S. A. Haque, T. Lutz, and J. R. Durrant, J. Am. Chem. Soc. **125**(2), 475 (2003).
[16] C. Prasittichai, J. R. Avila, O. K. Farha, and J. T. Hupp, J. Am. Chem. Soc. **135**(44), 16328 (2013).
[17] A. K. Chandiran, M. K. Nazeeruddin, and M. Gratzel, Adv. Funct. Mater. **24**(11), 1615 (2014).
[18] M. J. Katz, M. J. D. Vermeer, O. K. Farha, M. J. Pellin, and J. T. Hupp, Langmuir **29**(2), 806 (2013).
[19] M. J. DeVries, M. J. Pellin, and J. T. Hupp, Langmuir **26**(11), 9082 (2010).
[20] C. Prasittichai and J. T. Hupp, J. Phys. Chem. Lett. **1**(10), 1611 (2010).
[21] F. Fabregat-Santiago, J. Garcia-Canadas, E. Palomares, J. N. Clifford, S. A. Haque, J. R. Durrant, G. Garcia-Belmonte, and J. Bisquert, J. Appl. Phys. **96**(11), 6903 (2004).
[22] Alan D. McNaught and Andrew Wilkinson, *IUPAC Compendium of Chemical Terminology* (Blackwell Scientific Publications, Oxford, 1997).
[23] See supplementary material at http://dx.doi.org/10.1063/1.4895038 for experimental details, absorption spectrum of bulk $CH_3NH_3PbI_3$, fraction, size, absorption spectrum, work function of unconverted PbI_2, and average photovoltaic performance.